BOR DERGİSİ
JOURNAL OF BORON
http://dergipark.gov.tr/boron

# Synthesis of $VB_2$-$V_3B_4$-$V_2B_3$/VC hybrid powders via powder metallurgy processes

**Duygu Ağaoğulları[1]*, Özge Balcı[2], Sıddıka Mertdinç[3], Emre Tekoğlu[4], M. Lütfi Öveçoğlu[5]**

[1]Istanbul Technical University, Faculty of Chemical and Metallurgical Engineering, Department of Metallurgical and Materials Engineering, Particulate Materials Laboratories (PML), 34469 Maslak, Istanbul, Turkey, ORCID ID orcid.org/0000-0002-0623-5586

[2]Koç University, Department of Chemistry, Rumelifeneri, 34450 Sarıyer, Istanbul, Turkey, ORCID ID orcid.org/0000-0001-6756-3180

[3]Istanbul Technical University, Faculty of Chemical and Metallurgical Engineering, Department of Metallurgical and Materials Engineering, Particulate Materials Laboratories (PML), 34469 Maslak, Istanbul, Turkey, ORCID ID orcid.org/0000-0002-2376-2062

[4]Istanbul Technical University, Faculty of Chemical and Metallurgical Engineering, Department of Metallurgical and Materials Engineering, Particulate Materials Laboratories (PML), 34469 Maslak, Istanbul, Turkey, ORCID ID orcid.org/0000-0003-1219-6226

[5]Istanbul Technical University, Faculty of Chemical and Metallurgical Engineering, Department of Metallurgical and Materials Engineering, Particulate Materials Laboratories (PML), 34469 Maslak, Istanbul, Turkey, ORCID ID orcid.org/0000-0002-1536-4961

**ARTICLE INFO**

**Article history:**
Received 05 July 2018
Revised form 13 October 2018
Accepted 17 October 2018
Available online 30 November 2018

**Research Article**

**DOI: 10.30728/boron.441148**

**Keywords**:
Annealing,
Mechanical milling,
Microstructure,
Vanadium borides,
Vanadium carbide.

**ABSTRACT**

The present study reports the *in-situ* synthesis of hybrid powders containing vanadium borides ($VB_2$, $V_3B_4$ and $V_2B_3$) and vanadium carbide (VC) using powder metallurgy methods. $VB_2$-$V_3B_4$-$V_2B_3$/VC hybrid powders were synthesized from $V_2O_5$, $B_2O_3$ and C powder blends via a carbothermal reduction route assisted by mechanical milling. Powder blends were mechanically milled up to 5 h in a high-energy ball mill. The milling process reduced the crystallite size, increased the uniformity of the particle distribution and hence increased the reactivity of the starting powders. As-blended and milled powders were annealed at different temperatures (1400, 1500 and 1600°C) for 12 h to investigate the probability of achieving vanadium boride and carbide phases simultaneously. Annealed powders were characterized using X-ray diffractometer (XRD), scanning electron microscope/energy dispersive spectrometer (SEM/EDS) and particle size analyzer. In case of using annealing temperature of 1400°C, $VB_2$-$V_3B_4$-$V_2B_3$/VC hybrid powders were obtained with an amount of unreacted $V_2O_5$. Annealing temperatures of 1500 and 1600°C resulted in the formation of $VB_2$, $V_3B_4$, $V_2B_3$ and VC phases. Milling affected the weight percentages of the phases as well as the type of major boride phase.

## 1. Introduction

Borides of IVB and VB group metals are known as transition metal borides which have high melting point, high hardness, high wear resistance and good chemical stability. Transition metal borides are generally used in high temperature applications, and wear and corrosion resistance required applications due to their superior thermal and mechanical properties [1, 2]. Vanadium borides consist of six stable phases ($V_3B_2$, VB, $V_5B_6$, $V_3B_4$, $V_2B_3$ and $VB_2$, stability degree increases from left to right) according to the binary phase diagram of V and B [1]. Direct combination of boron with vanadium, mechanical milling, borothermic and carbothermic reductions, solid-state reaction between vanadium chloride and $MgB_2$, $NaBH_4$ or $LiBH_4$, self-propagating high temperature synthesis and autoclave synthesis from $VCl_4$, $NaBH_4$ and Mg are the some synthesis methods for vanadium borides [1, 3, 4].

Not only transition metal borides but also transition metal carbides have superior properties such as high melting point, high hardness, high temperature strength, good electrical and thermal conductivities and high chemical and thermal stabilities [5-9]. Carbides of the transition metals have received considerable attention due to these properties, therefore they are widely used in many applications like cutting tools, high temperature materials, electronics, catalysts, etc. [5, 6, 9]. Among the transition metal carbides, vanadium carbides are potentials for automobile and aircraft engine materials because it blocked the grain growth and used as reinforcement together with their other excellent properties [10]. Vanadium carbides include four stable phases (VC, α-$V_2C$, β-$V_2C$ and $V_4C_3$) and two metastable phases ($V_6C_5$ and $V_8C_7$) [11]. Vanadium carbides have been synthesized using various methods such as chemical vapour deposition, mechanical alloying, gas reduction-carburization, temperature programmed reactions, etc. [8, 9].

Addition of a second phase develops the mechanical properties such as fracture toughness and strength of a single phase ceramic materials [12]. Additionally, boride/carbide hybrid ceramics may exhibit improved mechanical properties than their individual characteristics. Along the all production methods of vanadium

*Corresponding author: bozkurtdu@itu.edu.tr

boride and carbide, mechanical milling assisted annealing process can be used for the production of boride/carbide hybrid powders [13]. Milling process provides the mechanical activation of the powders and subsequent annealing enables the activated particles to react at lower temperatures than that of thermodynamically required [14, 15].

In this study, in-situ synthesis of vanadium boride/vanadium carbide hybrid powders was presented. The reaction between the raw materials of $V_2O_5$, $B_2O_3$ and C enables to the simultaneous formation of boride and carbide phases by means of mechanical milling assisted carbothermal reduction. The effects of milling time and annealing temperature on the synthesized hybrid powders were investigated. Due to the fact that the preparation of vanadium boride/carbide powders is not a well-discussed topic and there is still an open area here, this study will contribute to the archival literature with its leading results.

## 2. Materials and method

Vanadium oxide ($V_2O_5$, Alfa Aesar™, 99.6 % purity, 300 µm average particle size), boron oxide ($B_2O_3$, ETI Mine, 98 % purity, 470 µm average particle size) and graphite (C, Alfa Aesar™, 99 % purity, 45 µm average particle size) powders were used as raw materials. Powder blends containing the stoichiometric amounts of raw materials were prepared based on the theoretical reduction reaction given in Eq.(1). The rationale for the utilization of Eq.(1) is to believe the yield of boride and carbide phases as solid reaction products together with CO gas. The reactant powders were mixed in a WAB™ T2C Turbula blender for 30 min to prepare as-blended powders.

$$V_2O_{5(s)} + 2\,B_2O_{3(s)} + 11\,C_{(s)} = 2\,VB_{2(s)} + 11\,CO_{(g)} \quad (1)$$

High-energy ball milling experiments were performed by using a Spex™ 8000 D Mixer/Mill (1200 rpm). Hardened steel vials (capacity: 50 ml) and hardened steel balls (diameter: 6 mm) were used with a 10:1 ball-to-powder weight ratio (BPR). Two different milling times (1 and 5 h) were applied to powder blends. Milling vials were filled with powders under Ar (Linde™, 99.999 % purity) atmosphere in the Plaslabs™ glove box. Both as-blended and milled powders placed in alumina boats were annealed in a horizontal tube furnace (Protherm™) at 1400, 1500 and 1600°C for 12 h under flowing Ar gas with a heating and cooling rate of 10°C/min.

Crystalline phases of the as-blended, milled and annealed powders were identified using a Bruker™ D8 Advanced Series X-ray diffractometer (XRD) with $CuK_\alpha$ (1.54060 Å) radiation, and 35 kV/40 mA operating conditions. International Centre for Diffraction Data (ICDD) powder diffraction database was utilized for crystalline phase determinations. Also, the crystallite sizes and lattice deformations of $V_2O_5$ and C were determined using Bruker-AXS TOPAS V4.2 software in regard of XRD patterns. The amounts of the phases in the milled and/or annealed powders were calculated by the semi-quantitative Rietveld method. Fourier transform infrared (FTIR) spectrum of the powders were recorded by using a Perkin Elmer™ Spectrum 100 FTIR at wavenumber ranging between 1000 and 4000 $cm^{-1}$ by using KBr pellet technique. Additionally, thermal analysis of the powders was examined by a TA™ Instruments Q600 differential scanning calorimeter (DSC) up to 1000°C with 10°C/min heating and cooling rates, under Ar atmosphere. Powder morphologies were characterized using a Quanta FEI™ FEG 250 scanning electron microscope (SEM). Elemental mapping analysis was conducted with EDS detector equipped to JEOL™ NeoScope JCM6000 Plus SEM. The average particle sizes of the powders were measured in distilled water using a Microtrac™ Nano-flex particle size analyzer (PSA) equipped with a Bandelin Sonopuls™ ultrasonic homogenizer.

## 3. Results and discussion

XRD patterns of the as-blended, 1 and 5 h of milled $V_2O_5$ and C powders are given in Figure 1. There is no evidence of the formation of new phases during milling up to 5 h (Figure 1). Only $V_2O_5$ (ICDD card number = 01-089-2483) and C (ICDD card number = 00-056-0159) phases are detected in the XRD analyses of the as-blended powders and those milled for 1 and 5 h. Although, $B_2O_3$ was used as starting material, there was no peak belonging to $B_2O_3$ due to its amorphous structure [13]. Presence of the $B_2O_3$ is determined by FTIR analysis, and FTIR spectra of the both as-blended and 5 h of milled samples were given in Figure 2. B-O deformation and stretching modes are seen clearly near 1200 and 1400 $cm^{-1}$, respectively [13, 16]. Additionally, physically or chemically adsorbed humidity on the surfaces of the powders leads to the formation of B-H (at about 2275 $cm^{-1}$) and B-OH bonds (at about 3250 $cm^{-1}$) [17]. Additionally, as seen from Figure 2, intensities of the FTIR peaks decreased after milling which is in good agreement with the corresponding XRD pattern in Figure 1.

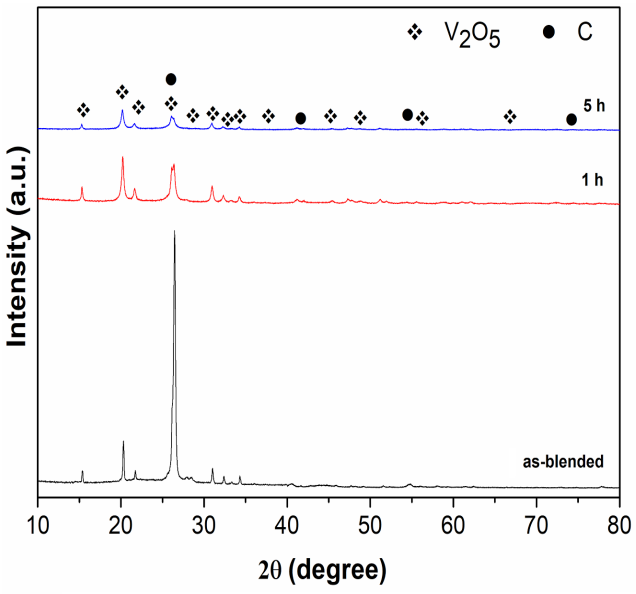


**Figure 1.** XRD patterns of the as-blended, 1 and 5 h of milled $V_2O_5$-$B_2O_3$-C powders.

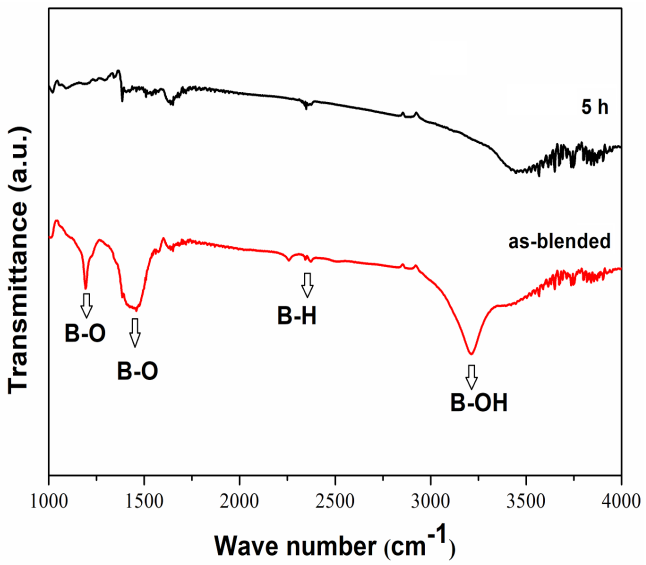


**Figure 2.** FTIR spectra of the as-blended and 5 h of milled $V_2O_5$-$B_2O_3$-C powders.

Figure 3 shows the TGA curve of the 5 h of milled powders in order to detect the weight loss or weight gain behaviour of the sample. As expected, 5 h of milled powders lost approximately 2.25 % of its weight up to 1000°C because of its C content. The initial C converted to CO gas by the effect of heat and CO gas release resulted in the weight loss.

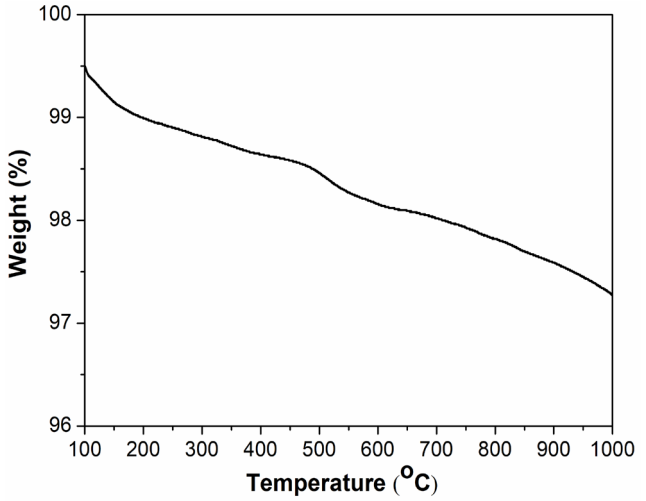


**Figure 3.** TGA curve belonging to the 5 h of milled $V_2O_5$-$B_2O_3$-C powders.

Furthermore, intensities of the XRD peaks decreased and peaks broadened by increasing milling time from 1 to 5 h (Figure 1). This intensity decline figures out the increasing lattice deformations and decreasing crystallite sizes during milling. Average lattice deformation and crystallite size values were calculated via TOPAS software based on the XRD patterns, and results are given in Table 1. The average crystallite sizes and lattice strains were determined using the most intense three $V_2O_5$ peaks. As seen in Table 1, average crystallite size sharply reduces, and average lattice strain dramatically increases after milling for 1 h due to high deformation. After milling for 5 h, smallest crystallite size (15.45 nm) and highest lattice deformation (4.123 %) were achieved.

Figures 4a-e show the SEM image and elemental mappings (V, B, C and O) of the as-blended $V_2O_5$-$B_2O_3$-C powders, respectively. Figure 4a illustrates the irregular shaped initial powders with different morphologies and particle sizes. The elemental V and B mappings (Figures 4b and 4c) show the distributions of the $V_2O_5$ and $B_2O_3$ phases. Since the initial size of the graphite particles is smaller than the other starting powders, small particles shown in Figure 4a can be C as compatible with the C regions in Figure 4d. Additionally, as seen in Figure 4e, O distributed homojeneously into the microstructure due to the presence of $V_2O_5$ and $B_2O_3$.

SEM image and elemental mapping results of the 5 h of milled powders are illustared in Figures 5a-e. Dissimilar to the microstructure in Figure 4a, 5 h milled powders show an agglomerated morphology with reduced particle sizes (Figure 5a). As seen in Figures 5b-e, V, B, O and C distributed uniformly throughout the microstructure after 5 h of milling due to the effective mixing and grinding which result in a significant degree of particle size reduction.

Figure 6 shows the DSC thermogram belonging to the 5 h of milled $V_2O_5$-$B_2O_3$-C powders. According to the curve, there is a large heat flow decrease between the temperatures of 500 and 1000°C. This decrease is related with the CO gas release as previously shown in Figure 3. After heating above 1000°C, a shallow and broad exotherm peaking at about 1150°C emerged. Also there is a heat flow increase between 1300 and 1400°C. However the following step can not be detected by the utilized DSC instrument because its heating capacity is not capable over 1400°C. Both the exotherm and heat flow increase can be attributed to the formation of new phases by carbothermal reduction of $V_2O_5$ and $B_2O_3$ reactants. It should be also noted that the DSC heating of the milled powders is beneficial for determining the annealing temperature to initiate the chemical reaction. Thus, annealing at 1400°C and above is chosen to obtain V boride and carbide phases.

**Table 1.** Average crystallite sizes and lattice strains of the $V_2O_5$ phase in the as-blended $V_2O_5$-$B_2O_3$-C powders and those milled for 1 and 5 h.

| Milling time | Average crystallite size (nm) | Average lattice strain (%) |
|---|---|---|
| As-blended | 250.90 | 0.312 |
| 1 h | 80.60 | 2.345 |
| 5 h | 15.45 | 4.123 |

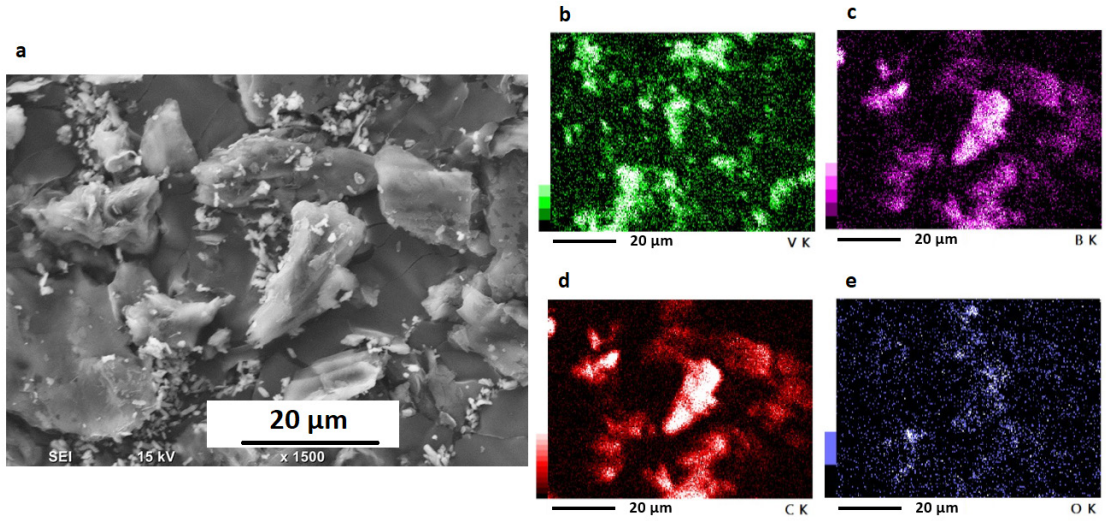


**Figure 4.** SEM and EDS analyses of the as-blended $V_2O_5$-$B_2O_3$-C powders: (a) SEM image and (b-e) respective EDS mappings for V, B, C and O elements.

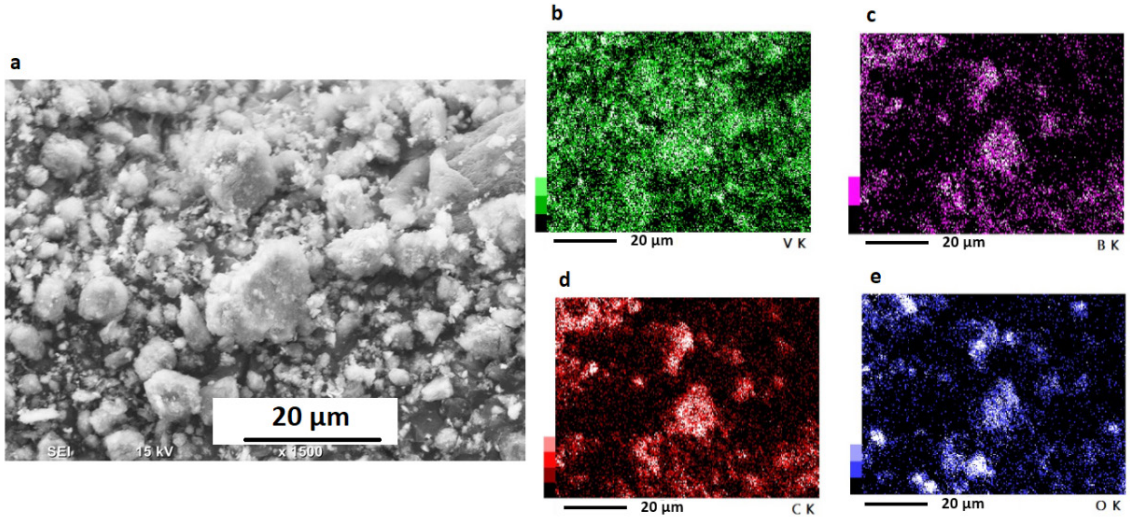


**Figure 5.** SEM and EDS analyses of the 5 h of milled $V_2O_5$-$B_2O_3$-C powders: (a) SEM image and (b-e) respective EDS mappings for V, B, C and O elements.

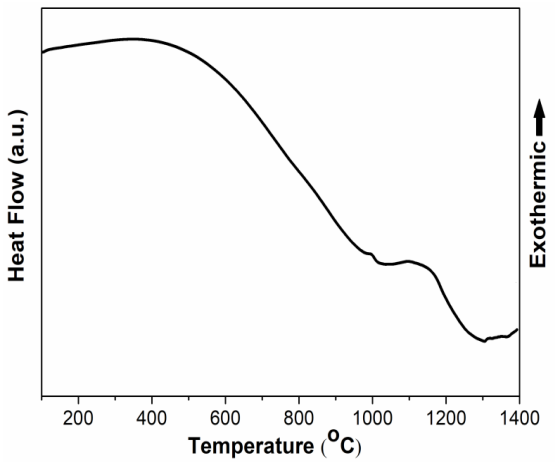


**Figure 6.** DSC thermogram belonging to the 5 h of milled $V_2O_5$-$B_2O_3$-C powders.

Figures 7a-b display the XRD patterns of the as-blended $V_2O_5$-$B_2O_3$-C powders after annealing at 1500°C and 1600°C for 12 h, respectively. Both annealed powders have the phases of $V_2B_3$ (ICDD card number = 01-083-0172), $V_3B_4$ (ICDD card number = 00-009-0321), $VB_2$ (ICDD card number = 00-038-1463) and VC (ICDD card number = 03-065-8074) phases. The composition of the powders annealed at 1500°C (Figure 7a) is 39.8 wt.% $V_2B_3$, 23.5 wt.% $V_3B_4$, 15.7 wt.% $VB_2$ and 21 wt.% VC. Besides, the powders annealed at 1600°C (Figure 7b) include the chemistry of 43.2 wt.% $V_2B_3$, 17.1 wt.% $V_3B_4$, 14.4 wt.% $VB_2$ and 25.3 wt.% VC. When annealing temperatures are compared with each other, it can be said that an increase of 100°C increases the weight percentages of $V_2B_3$ and VC phases. It should be also noted that although V boride ($V_2B_3$, $V_3B_4$, $VB_2$) and carbide phases are obtained after annealing of the as-blended powders, $VB_2$ which is the most stable V boride phase is found at the lowest amount in the overall powder.

XRD patterns of the 5 h of milled powders and those annealed at 1400, 1500 and 1600°C are presented in Figures 8a-c, respectively. XRD pattern of the powders milled for 5 h and annealed at 1400°C consist of the peaks of $VB_2$, $V_2B_3$, $V_3B_4$ and VC phases in addition to a small amount of unreacted $V_2O_5$ phase. Since all $V_2O_5$

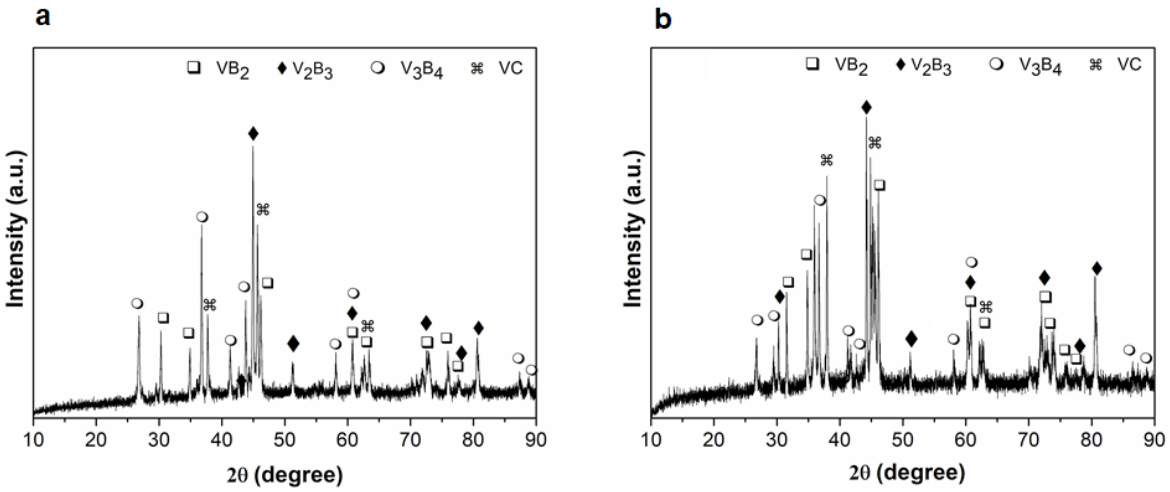


**Figure 7.** XRD patterns of the as-blended $V_2O_5$-$B_2O_3$-C powders after annealing at (a) 1500°C and (b) 1600°C for 12 h.

did not participate into the reaction and an amount of it left behind, it can be said that initial materials did not completely transform to the V borides and carbide at 1400°C. As seen in Figure 8b, vanadium boride ($VB_2$, $V_2B_3$, $V_3B_4$) and vanadium carbide (VC) phases formed after annealing at 1500°C, without the presence of unreacted $V_2O_5$. Also, semi-quantitative Rietveld analysis shows that the powders annealed at 1500°C have the chemistry of 54.8 wt.% $VB_2$, 20.8 wt.% $V_2B_3$, 12.3 wt.% $V_3B_4$ and 12.1 wt.% VC. Same phases were also detected in the powders annealed at 1600°C (Figure 8c). According to the Rietveld calculations, the amounts of the $VB_2$, $V_2B_3$, $V_3B_4$ and VC phases in the powders annealed at 1600°C are 56.5 wt.%, 24.2 wt.%, 10.2 wt.% and 9.1 wt.%, respectively. Due to the fact that the most stable phase of the V-B binary system is $VB_2$, the amounts of the $VB_2$ and $V_2B_3$ phases increase and the amount of $V_3B_4$ phase decreases as the annealing temperature changed from 1500 to 1600°C. Moreover, it can be stated that 5 h of milling resulted in a composition change of the hybrid powders. Milling increased the number of active and fresh surfaces in the powders, provided a homogeneous dispersion of the reactants and hence increased the probability of yielding the most stable V-B phase as the major compound.

Particle size distributions of the 5 h of milled powders and those annealed at various temperatures are given in Figures 8d-f. Particle size distribution of the powders milled for 5 h and annealed at 1400°C is not so homogeneous and show a large histogram between 100 and 1000 nm with two peaking points (Figure 8c). Average particle size of this powder is measured as 553 nm. The most homogeneous particle size distribution with a mono modal histogram is seen for the powders annealed at 1500°C, exhibiting an average particle size value of 620 nm (Figure 8d). As expected, an increase in the annealing temperature (100°C) also increased the particle size of the powders. On the other hand, powders annealed at 1600°C have a

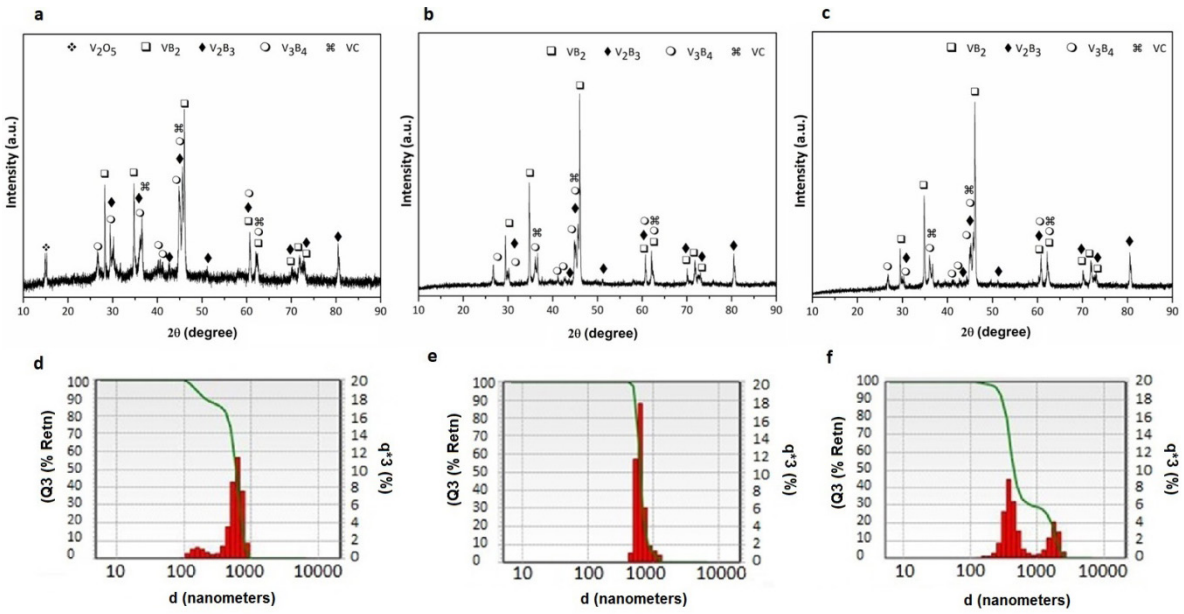


**Figure 8.** XRD patterns and particle size distributions of the $V_2O_5$-$B_2O_3$-C powders milled for 5 h and annealed at (a,d) 1400°C, (b,e) 1500°C and (c,f) 1600°C for 12 h.

bimodal particle size distribution with an average particle size of 803 nm (Figure 8f). Annealing temperature of 1600°C resulted in higher particle size value due to grain growth by the effect of heat.

Figure 9 presents the SEM image (Figure 9a) and EDS analyses (Figures 9b-e) of the powders milled for 5 h and annealed at 1500°C for 12 h. Microstructure of the powders exhibits submicron particles with equiaxed morphologies (Figure 9a). Formation of the V boride and carbide phases after annealing changed the morphology of the milled powders, as compared to Figure 5a. Additionally, elemental mappings taken from the general SEM image in Figure 9b show that V, B and C elements dispersed throughout the microstructure (Figures 9c-e), indicating the presence of V borides and VC.

Figure 10a shows the SEM image of the powders milled for 5 h and annealed at 1600°C for 12 h. Irregular shaped particles with submicron sizes are clearly seen. After annealing, particle coalescence occurred which is obviously different from the microstructure of the milled powders (Figure 5a). Similar morphological changes during annealing were previously observed during the microstructural analyses of the annealed $Nb_2O_5$-$B_2O_3$-C powders reported in the study of Balcı et al. [13]. Based on the SEM image given in Figure 10(b), V, B and C elemental mappings were (Figures 10c-e). V elemental maps clearly indicate the uniform distributions of the V through the microstructure. B and C mapping images show the distribution of the B and C located at the same regions (Figures 10d-e). Therefore, these regions contain both vanadium boride and vanadium carbide phases in the sample volume.

Figures 11a-b are the respective FTIR spectra of the powders 5 h of milled and annealed at 1500°C and 1600°C. FTIR spectra can be a solid proof of the absence of oxide-related compounds (unreacted $B_2O_3$, $H_3BO_3$, etc.) in the annealed samples. However, any peak showing a significant transmittance was not detected for the both annealed powders [18-20]. This corresponded that the 5 h of milled and annealed samples are hybrid powders only containing $VB_2$, $V_2B_3$, $V_3B_4$ and VC phases without any impurity.

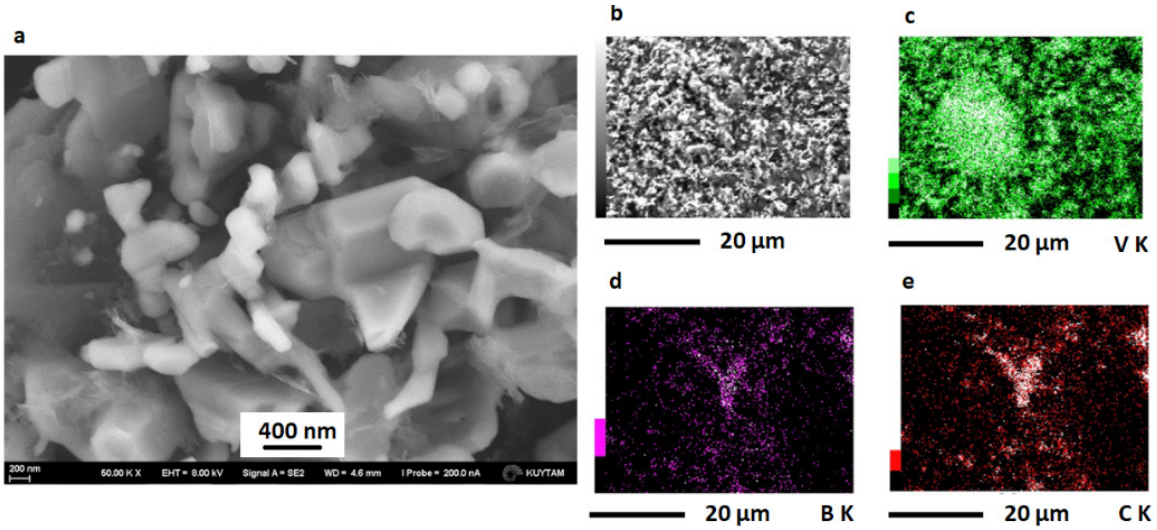


**Figure 9.** (a) SEM image and (b-e) EDS analyses of the $V_2O_5$-$B_2O_3$-C powders milled for 5 h and annealed at 1500°C.

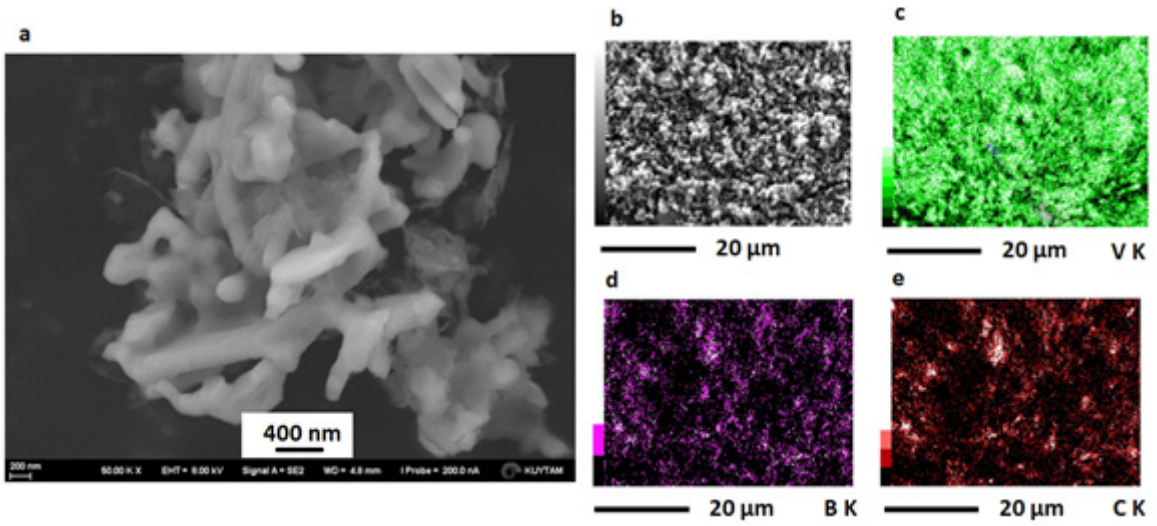


**Figure 10.** (a) SEM image and (b-e) EDS analyses of the $V_2O_5$-$B_2O_3$-C powders milled for 5 h and annealed at 1600°C.

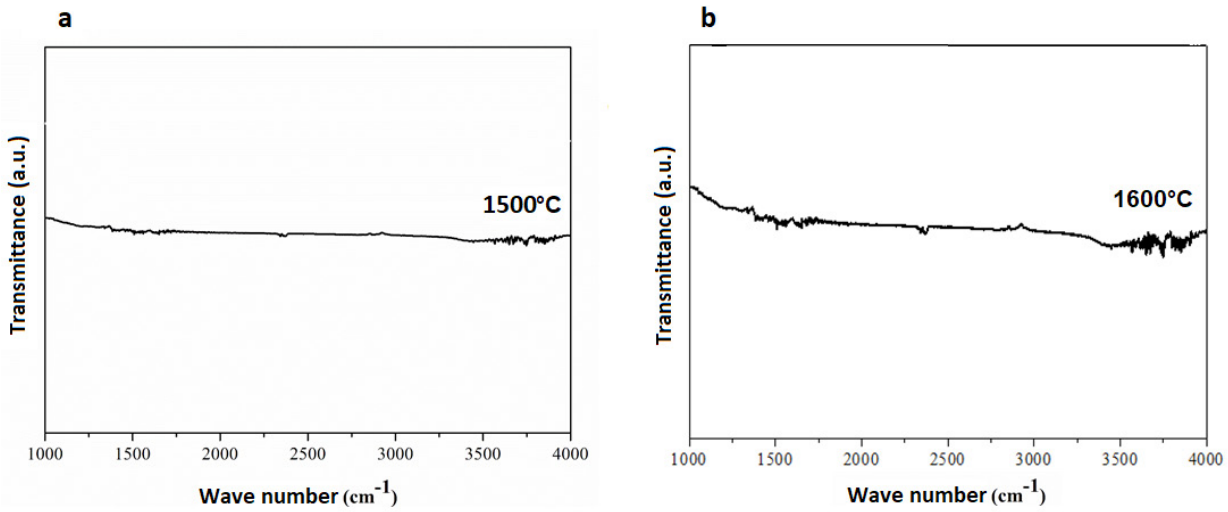


**Figure 11.** FTIR spectra of the 5 h milled $V_2O_5$-$B_2O_3$-C powders and those annealed at (a) 1500°C and (b) 1600°C.

Consequently, this study shows the *in-situ* synthesis of $VB_2/V_3B_4/V_2B_3$/VC hybrid powders using powder metallurgy methods such as mechanical milling and annealing. The lack of an additional purification step to reach pure reaction products can be also evaluated as an advantage of this process. The difference of blending and milling carried out prior to the annealing was observed in terms of product stoichiometry. The synthesis of hybrid powders at various weight percentages of $VB_2$, $V_3B_4$, $V_2B_3$ and VC phases by using powder metallurgy methods and by controlling limited amount of process parameters can be an alternative way to prepare powder precursors for some potential application areas.

## 4. Conclusions

In this study, *in-situ* synthesis of hybrid powders containing vanadium borides ($VB_2$, $V_3B_4$ and $V_2B_3$) and vanadium carbide (VC) was carried out via mechanical milling and annealing processes.

Based on the performed analyses, the following results can be summarized:

- Mechanical milling resulted in a homogeneous distribution of the reactants as well as particle size reduction and activation.
- Both as-blended and milled stoichiometric $V_2O_5$-$B_2O_3$-C powder blends yielded vanadium boride and carbide phases after annealing, dissimilar to the theoretical reduction reaction.
- The products annealed after blending and mechanical milling had different stoichiometry.
- Mechanical milling prior to annealing resulted in an increase in the amount of the most stable vanadium boride phase ($VB_2$).
- An increase in the annealing temperature increases the average particle sizes of the hybrid powders and changes the weight percentages of the phases.
- Submicron scaled $VB_2/V_3B_4/V_2B_3$/VC hybrid powders were obtained free of any impurity.

## References

[1] Yeh C. L., Wang H. J., Combustion synthesis of vanadium borides, J. Alloys Compd., 509, 3257–3261, 2011.

[2] Shi F., Wang L., Liu J., Synthesis and characterization of silica aerogels by a novel fast ambient pressure drying process, Mater. Lett., 60, 3718–3722, 2006.

[3] Hassanzadeh-Tabrizi S. A., Davoodi D., Beykzadeh A. A., Salahshour S., Fast mechanochemical combustion synthesis of nanostructured vanadium boride by a magnesiothermic reaction, Ceram. Int., 42, 1812–1816, 2016.

[4] Shi L., Gu Y., Chen L., Yang Z., Ma J., Qian Y., Low-temperature synthesis of nanocrystalline vanadium diboride, Mater. Lett., 58, 2890–2892, 2006.

[5] Zhao Z., Liu Y., Cao H., Gao S., Tu M., Synthesis of vanadium carbide nanopowders by thermal processing and their characterization, Powder Technol., 181, 31–35, 2008.

[6] Ma J., Wu M., Du Y., Chen S., Ye J., Jin L., Low temperature synthesis of vanadium carbide (VC), Mater. Lett., 63, 905–907, 2009.

[7] Zhang B., Li Z.Q., Synthesis of vanadium carbide by mechanical alloying, J. Alloys Compd., 392, 183–186, 2005.

[8] Wu Y. D., Zhang G. H., Chou K. C., A novel method to synthesize submicrometer vanadium carbide by temperature programmed reaction from vanadium pentoxide and phenolic resin, Int. J. Refract. Met. Hard Mater., 62, 64–69, 2017.

[9] Hossein-Zadeh M., Razavi M., Safa M., et. al., Synthesis and structural evolution of vanadium carbide in nano scale during mechanical alloying, J. King Saud Univ. Eng. Sci., 28, 207–212, 2016.

[10] Kurlov A. S., Gusev A. I., Gerasimov E. Y., Bobrikov I. A., Balagurov A. M., Rempel A. A., Nanocrystalline or-

dered vanadium carbide: Superlattice and nanostructure, Superlattices Microstruct., 90, 148–164, 2016.

[11] Lipatnikov V. N., Phase equilibria, phases and compounds in the V–C system, Russ. Chem. Rev., 74, 697–723, 2005.

[12] Mestral F., Thevenot F., Ceramic composites: $TiB_2$-TiC-SiC - Part I Properties and microstructures in the ternary system, J. Mater. Sci., 26, 5547–5560, 1991.

[13] Balcı Ö., Ağaoğulları D., Ovalı D., Öveçoğlu M. L., Duman İ., In situ synthesis of $NbB_2$-NbC composite powders by milling-assisted carbothermal reduction of oxide raw materials, Adv. Powder Technol., 26, 1200–1209, 2015.

[14] Balcı Ö., Ağaoğulları D., Duman İ., Öveçoğlu M. L., Carbothermal production of $ZrB_2$–$ZrO_2$ ceramic powders from $ZrO_2$–$B_2O_3$/B system by high-energy ball milling and annealing assisted process, Ceram. Int., 38, 2201–2207, 2012.

[15] Suryanarayana C., Mechanical alloying and milling, Prog. Mater Sci., 46, 1–184, 2001.

[16] Balachander L., Ramadevudu G., Shareefuddin M., Sayannac R., Venudharc Y. C., IR analysis of borate glasses containing three alkali oxides, Sci. Asia, 39, 278–283, 2013.

[17] Moon O. M., Kang B. C., Lee S. B, Boo J. H. Temperature effect on structural properties of boron oxide thin films deposited by MOCVD method, Thin Solid Films, 464–465, 164–169, 2004.

[18] Krutskii Y. L., Maksimovskii E. A., Krutskaya T. M., Popov M. V., Netskina O. V., Nikulina A. A., Cherkasova N. Yu., Kvashina T. S., Synthesis of highly dispersed vanadium diboride with the use of nanofibrous carbon, Russ. J. Appl. Chem., 90, 1379–1385, 2017.

[19] Grigor O. N., Koval V. V., Zaporozhets O. I., Bega N. D., Galanov B. A., Prilutskii É. V., Kotenko V. A., Kutran T. N., Dordienk N. A., Synthesis and Physicomechanical Properties of $B_4C - VB_2$ Composites, Powder Metall. Met. Ceram., 45, 47–58, 2006.

[20] Demirskyi D., Sakka Y., Vasylkiv O., Consolidation of $B_4C$-$VB_2$ eutectic ceramics by spark plasma sintering, J. Ceram. Soc. Jpn., 123,1051–1054, 2015.